

# Negative differential resistance in C<sub>60</sub> Diodes

Philipp Stadler<sup>1</sup>, Anita Fuchsbauer<sup>1</sup>, Günther Hesser<sup>2</sup>, Thomas Fromherz<sup>3</sup>,  
Gebhard J. Matt<sup>1</sup>, Helmut Neugebauer<sup>1</sup> and Serdar N. Sariciftci<sup>1</sup>

<sup>1</sup> Linz Institute for Organic Solar Cells, Physical Chemistry, Johannes Kepler University  
Linz, Altenbergerstraße 69, 4040, Austria

E-mail: philipp.stadler@jku.at

<sup>2</sup> Technische Service Einheit (TSE), Johannes Kepler University Linz, Altenbergerstraße  
69, 4040 Linz, Austria

E-mail: guenther.hesser@jku.at

<sup>3</sup> Institute for Semiconductor and Solid State Physics, Johannes Kepler University Linz,  
Altenbergerstraße 69, 4040, Austria

E-mail: thomas.fromherz@jku.at

**Abstract.** Morphology studies and current-voltage (*IV*) measurements of C<sub>60</sub> thin film diodes in the temperature range of 300 – 4.2 K are presented. For defined evaporation parameters orientation domains along the growth direction are demonstrated by cross section transmission electron microscopy. From the electrical characterization the fullerene diodes exhibit space charge limited currents which follow a power law dependency. At current densities above 100 mA cm<sup>-2</sup> and temperatures below 200 K reversible voltage instabilities (S-shape *IV* characteristics, negative differential resistance) arise. The instabilities are similar to charge transport effects in amorphous inorganic semiconductors.

## 1. Introduction

Fullerene and its derivatives are dominantly used as electron acceptor molecules in conducting polymer matrices for solar cells. The investigation of the transport properties of these materials are therefore of importance. Here we concentrate on the properties of C<sub>60</sub> films processed by thermal evaporation in sandwich type diodes [1]. The high purity and reproducibility in thin films grown by evaporation allow the study of both, the transport properties as well as the morphology of these materials. The nature of charge transport in fullerenes and in amorphous or polycrystalline inorganic semiconductors is similar. In both cases charge injection follows the space charge limited current (SCLC) theory. With C<sub>60</sub>, a reversible voltage instability is observed at low temperatures corresponding to similar effects in amorphous inorganics [2,3]. The origin of the voltage breakdown is designated to charge trapping next to the electrodes, followed by the formation of conductive filaments in the bulk C<sub>60</sub> layer.

## 2. Experimental Methods

Sandwich-type diodes were fabricated using 70 nm thick poly(3,4-ethylenedioxythiophene/poly(styrene-sulfonate) (PEDOT:PSS) spin coated film on ITO glass as hole injection electrode. 300 nm  $C_{60}$  films were grown on top by thermal evaporation. The substrate temperature was kept constant at 140° C during the deposition process. The morphology studies were performed by transmission electron microscopy (TEM). For the transport measurements we used 50 nm Chromium layers as top contact. All electrical characterizations were performed in a Helium flow cryostat (Oxford Industries) in a temperature range between 300 K to 4.2 K. The voltage drop between the PEDOT:PSS and the Chromium electrode was measured by applying a certain current density to the diode.

## 3. Results

The device structure and the energy levels of the fullerene diode are shown in Figure 1. The estimated built-in voltage between the Fermi level of the Chromium (-4.5 eV) and the Fermi level of PEDOT:PSS (-5.2 eV) is about 0.7 V. The low energy of the HOMO of the  $C_{60}$  results in an energy barrier of around 0.6 eV for the hole injection which is comparatively higher than for the electron injection.

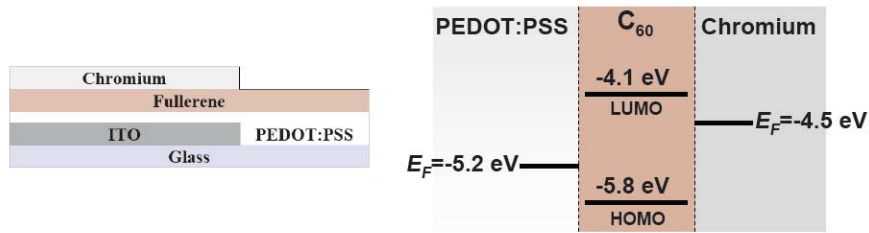


**Fig. 1.** Device sandwich – type structure and band diagrams of the  $C_{60}$  diode

The electrical characterization was performed in the high injection regime (forward direction, Chromium as cathode). For gaining the effective voltage drop the built-in potential ( $U_{\text{eff}} = U_{\text{measured}} - U_{\text{BI}}$ ) is subtracted from the measured voltage drop in the device. In Figure 2 the  $IV$  characteristics at 3 temperatures are shown.

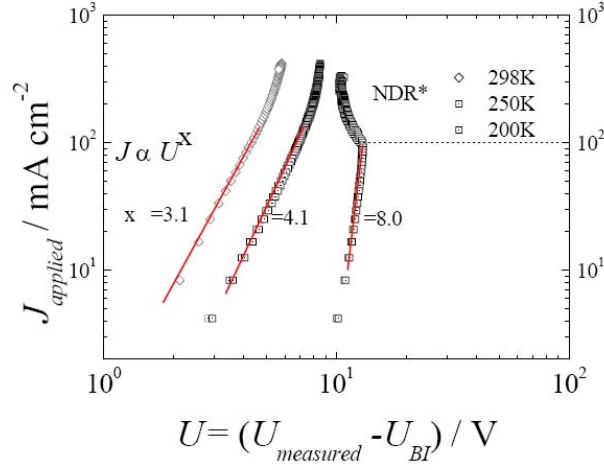


**Fig. 2.** Double logarithmic *IV* characteristics at 300 K, 250 K and 200 K.

The *IV* behaviour is described with a formation of a space charge upon the dominant electron-injection (space charge limited currents, SCLC). The current density follows a power law dependence, described with the Mott-Gurnier formula in (1)

$$J = \frac{9}{8} \cdot \Theta \cdot \varepsilon \cdot \mu \cdot \frac{V^2}{L^3} \quad \text{and} \quad \Theta = \frac{n_{\text{free}}}{n_{\text{injected}}} \quad (1)$$

where  $\mu$  is the mobility,  $L$  the thickness of the diode and  $\Theta$  the ratio of free to injected charge carriers. In ideal case (no traps) the ratio is close to 1 and the exponent is 2. In  $C_{60}$  the injection process is more complex due to presence of shallow and deep traps. We see experimentally a higher exponent (Fig. 2), since the factor  $\Theta$  is also voltage-dependent. As in many organic systems, also with evaporated  $C_{60}$  the morphology influences the transport properties. The cross section TEM studies verify high crystallinity of  $C_{60}$  and lateral faceted crystallite domains along the growth direction (Fig. 3). Trapping is present at crystallite grain boundaries and the free carrier concentration is dependent on the temperature and the morphology [4,5].

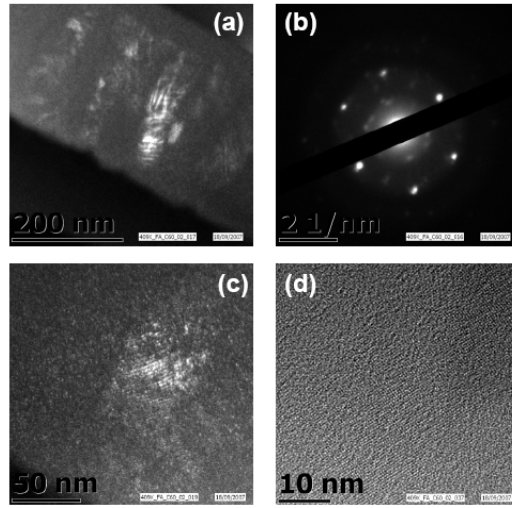


**Fig. 3.** (a) Dark-field analysis of diode cross section and zoom in (c) shows similar orientation domains in growth direction. (b) Diffraction pattern of  $C_{60}$  crystallite exhibits fcc hexagonal structure. (d) High resolution dark field shows orientation domain of the molecules.

The power law dependency is fulfilled when operating with current densities around  $100 \text{ mA cm}^{-2}$ . The exponent increases by decreasing the temperature, as seen in figure 2. At current densities above  $100 \text{ mA cm}^{-2}$  and temperatures below 200 K deviations from the SCLC behaviour are observed. By applying a higher current density the measured voltage decreases showing a negative-differential resistance (NDR) seen in figure 4.

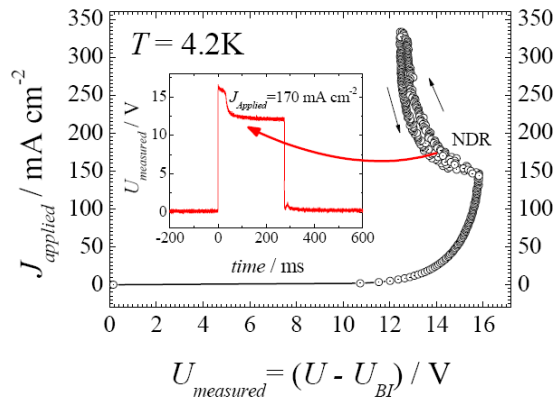


**Fig. 4.** Negative differential resistance regime at 4.2 K showing a reversible voltage breakdown. Inset: Voltage drop measured time-resolved in negative differential regime.

The *IV* forward and reverse scan exhibits a well pronounced negative differential resistance regime at 4.2 K above  $150 \text{ mA cm}^{-2}$ . Consequently we can exclude thermal effects as origin for the voltage breakdown. The inset plot in Figure 4 shows the measured voltage drop time resolved. In the first 20 ms of the current pulse the voltage remains at the value corresponding to a SCLC behaviour, then the voltage drops to a constant level until the end of the 250 ms current pulse.

#### 4. Conclusions

It is known that transport in  $C_{60}$  is influenced by the purity and crystallinity of the material. In this work the evaporation parameters are controlled in order to grow high quality films on the PEDOT:PSS anode. From the morphology studies in figure 3 the authors state that crystallites with similar oriented domains are formed in the growth direction. These films exhibit in the electrical transport characterization space charge limited (SCL) currents, which follow a power law dependency as expected from the theory. The current voltage characteristics from the diode correspond to the SCL current with presence of traps. At temperatures below 200 K and current densities above  $100 \text{ mA cm}^{-2}$  a reversible voltage instability arises. In analogy to amorphous inorganic semiconductors, this phenomena is described with the formation of conductive filaments in the bulk of the  $C_{60}$  film (injection over a non-uniform injection area). Since the high conductivity at low temperatures cannot be explained with a thermal activation process, we propose a band transport model and an existence of a mobility edge [6].

**Acknowledgements.** We gratefully acknowledge the Austrian FWF Project and the Austrian NFN Project for support.

#### References

- 1 H. Sitter, A. Andreev and N. S. Sariciftci, *Mol. Cryst. Liq. Cryst.*, **385**, 171 (2002).
- 2 G. J. Matt, T. Fromherz and N. S. Sariciftci, *Appl. Phys. Lett.*, **84**, 1570 (2004).
- 3 N. F. Mott, *Contemp. Phys.*, **10**, 125-138 (1969).
- 4 K. Rikitake, T. Akiyama and W. Takashima, *Synth. Met.*, **86**, 2357 (1997).
- 5 G. Krakow, N. M Rivera, and J. J. Cuomo, *Appl. Phys. A.*, **56**, 185-192 (1995).
- 6 G. J. Matt, T. Fromherz, H. Neugebauer, N. S. Sariciftci, *Electronic Properties of Novel Nanostructures*, 530 (2005).